DOI: 10.31265/atnrs.781

Controlling Well Leakage: Rheological and Operational Effects

Mahdi Izadi[1], Elizabeth Trudel[2] and Ian Frigaard[1]

[1]University of British Columbia, Vancouver, Canada
[2]University of British Columbia, Kelowna, Canada

ABSTRACT

Many hydrocarbon wells leak gas, due to shrinkage and other microannuli that typically form along the cement-casing and cement-formation interfaces. These microannuli are variable due to irregularities in the primary cementing process and other operational anomalies. Repair of such defects is via a process called squeeze cementing, that involves pumping a thin cement slurry into the microannulus under pressure. Trudel & Frigaard[1] developed a stochastic model of well leakage able to predict all but extreme (high and low) rates of leakage for a median well in British Columbia (BC), Canada, benchmarked against leakage rates observed in 2010-2019. Izadi *et al.*[2,3] have explored the effects of pumping (yield stress) slurries into these narrow irregular geometries, using a Monte-Carlo approach to account for the extreme variability. This enabled us to give probabilistic predictions of the likely effects of the squeeze cementing operation. Here we extend our analysis to different operational scenarios, showing how rheological effects can influence repair of the microannulus

INTRODUCTION

Wellbore leakage refers to the unwanted release of hydrocarbons to the surface through defects along the length of an oil or gas well. Either the gas is vented at the surface casing (SCVF) or the vent is closed, which often results in surface casing pressure (SCP) buildup and gas migration (GM) away from the well. High incidence rates are a concern from the perspective of restricting methane emissions globally and contaminating groundwater. Given that the permeability of cement is generally very low, observed leakage rates cannot be accounted for by seepage through the cement sheath. Instead, it is widely believed that gas flows to surface along microannular layers at the interface between the cement sheath and the casing or formation. These layers are attributed to a combination cement shrinkage and interface debonding, possibly caused by various well operations (e.g. thermal cycling, hydraulic fracturing).

Remediation of wellbore leakage is accomplished through the squeeze cementing operation. In squeeze cementing, the casing is perforated with a large number of evenly spaced holes. The area to be remediated is isolated, the cement slurry is pumped down the well and pressure is applied from above to drive the cement slurry through the holes into the formation and then laterally to fill any free space within the microannulus; see

Fig. 1a & b. The effectiveness of the squeeze cementing job relies on careful selection and preparation of the cement slurry so that it is appropriate for the size of defect present in the annulus[4], e.g. using microfine cements to reduce granular jamming risks. Also important is to identify the location of the influx, so that remediation can be performed above the hydrocarbon source and ideally in caprock.

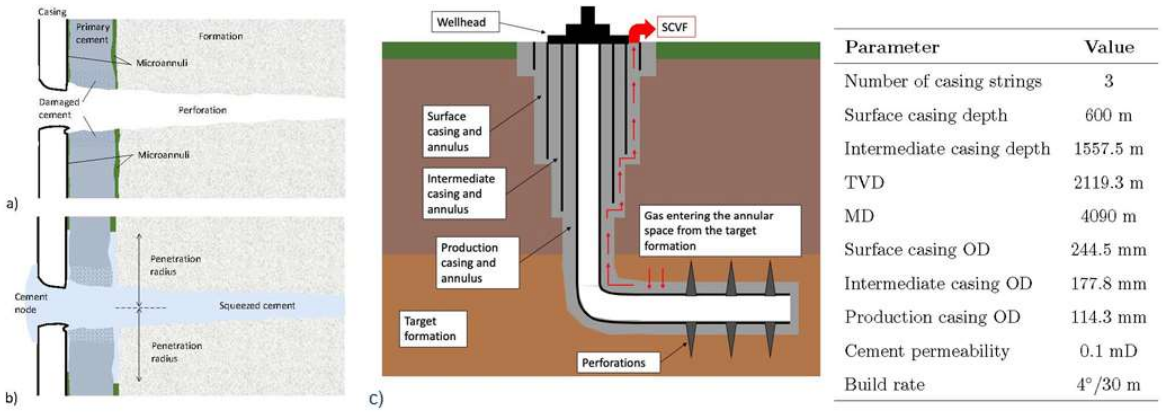

Parameter	Value
Number of casing strings	3
Surface casing depth	600 m
Intermediate casing depth	1557.5 m
TVD	2119.3 m
MD	4090 m
Surface casing OD	244.5 mm
Intermediate casing OD	177.8 mm
Production casing OD	114.3 mm
Cement permeability	0.1 mD
Build rate	4°/30 m

FIGURE 1: Schematic of the squeeze flow process: (a) & (b). In (c) we show characteristics of a typical well in British Columbia, used for the leakage model in Trudel & Frigaard[1,3].

Well leakage has become an important topic recently not only for productivity and emissions remediation. The past decade has seen a large growth in well decommissioning, both onshore[5] and offshore[6], which involves the use of cement plugs to seal inside the well. Concerns on sealing of wells also abound in considering depleted reservoirs for carbon capture and storage (CCS) operations, i.e. related to the potential leakage of CO_2. In these contexts a number of well leakage models have been advanced[7–13] and commonly the leakage potential of the well is modelled (or classified) by assigning either an *effective permeability* to the cemented annulus/plug, or assigning a uniform microannulus thickness, ranging between 5 to 300μm. Measurements of microannuli using CT scanning methods[14,15], visual inspection of lab-created microannuli[16,17] and observations from ultrasonic logging tools, all suggest that microannuli thickness can vary significantly azimuthally around the well and varies more slowly along the well.

The concern with uniform models is that they do not represent reality. For example, if such models are accepted as physical representations, it would not matter at which depth remediation work was performed. Some studies have directly taken CT measurements and simulated gas flow directly[18], which serve to emphasize the large variations in flow paths. Our approach[1] has been to stochastically construct microannuli that vary along the well and around the annulus in a way consistent with observations. For a given well architecture we then adopt a Monte-Carlo approach of creating a large number N of microannuli and computing the leakage flow through each. This gives a distribution of leakage flow rates, which can be used to calibrate the underlying model[1] and then explore a range of operational scenarios[19]. Such an approach and the inherent variability of the unknown leakage pathways helps explain the many challenges in predicting both leakage rate and remediation success.

Regarding remediation, there are few studies that model the detail of the squeeze

cementing operation. We believe this is largely due to the massive uncertainty of the operation. For example, the extent of perforated holes is unknown, the permeability/porosity of the far-field formation is poorly characterised, the microannular space is unknown and the effect of the perforation operation on damage zones behind the casing is unknown, as well as any cleanup/washing prior to cementing. Additionally, the precise cement slurry composition and rheology is not always carefully controlled or designed. Nevertheless, it is necessary to model this process in order to understand well leakage. To this end we have developed a physical model, based on modelling the cement slurry as a Herschel-Bulkley fluid and explored the invasion flows into typical microannuli geometries[2]. In Izadi *et al.*[3] this has been combined with our stochastic leakage model[1] and used to explore different squeeze cementing design parameters. Here we extend the underlying approach to new applications.

MODELLING THE INVASION FLOW

Squeeze cementing involves the penetration of the slurry into the narrow microannulus (MA) gap between the existing cement layer and either the casing or formation. We adopt our previous modelling approach for this flow[2]. The gap-averaged concentration of the slurry, $\bar{c}$, to leading order satisfies:

$$\frac{\partial}{\partial \hat{t}}[\hat{H}\bar{c}] + \hat{\nabla} \cdot [\hat{H}\bar{c}(\hat{\bar{u}}, \hat{\bar{v}})] = 0, \tag{1}$$

where $2\hat{H}(\hat{x}, \hat{y})$ is the height of the MA and $\hat{\nabla}$ operates only in the $(\hat{x}, \hat{y})$-plane. The concentration is used, together with the properties of both fluids, to define *mixture* rheological properties.

The gap-averaged velocity in $\hat{x}$ and $\hat{y}$ directions is $(\hat{\bar{u}}, \hat{\bar{v}})$, which can be defined in terms of a stream function $\hat{\psi}$:

$$\left(\frac{\partial \hat{\psi}}{\partial \hat{y}}, -\frac{\partial \hat{\psi}}{\partial \hat{x}}\right) = \int_0^{\hat{H}} (\hat{u}, \hat{v}) \; d\hat{z} = \hat{H}\left(\hat{\bar{u}}, \hat{\bar{v}}\right). \tag{2}$$

It can be shown[2] that $\left(\hat{\bar{u}}, \hat{\bar{v}}\right)$ is parallel to the pressure gradient $\hat{\nabla}\hat{p}$, flowing down the gradient. On integrating across the half-gap:

$$|\hat{\nabla}\hat{\psi}| = \frac{n\left(|\hat{\nabla}\hat{p}|\hat{H} - \hat{\tau}_y\right)_+^{1+\frac{1}{n}}\left((n+1)|\hat{\nabla}\hat{p}|\hat{H} + n\hat{\tau}_y\right)}{(n+1)(2n+1)\hat{\kappa}^{1/n}|\hat{\nabla}\hat{p}|^2}, \tag{3}$$

where $(\cdot)_+$ denotes the positive part of the bracketed expression. Here it is assumed that the fluid mixture locally has rheological properties described to leading order by the Herschel-Bulkley model, with yield stress $\hat{\tau}_y$, consistency $\hat{\kappa}$ and power law index n. In practice, it is the inverse of the expression in (3) that is used for computation, i.e. $|\hat{\nabla}\hat{p}| = \hat{S}(|\hat{\nabla}\hat{\psi}|)$, which can be written as:

$$\hat{S}(|\hat{\nabla}\hat{\psi}|) = \frac{\hat{\tau}_y}{\hat{H}} + \hat{\chi}(|\hat{\nabla}\hat{\psi}|). \tag{4}$$

The function $\hat{\chi}(|\hat{\nabla}\hat{\psi}|)$ represents the viscous part of the pressure gradient, i.e. once the critical pressure gradient $\hat{\tau}_y/\hat{H}$ has been exceeded.[20] Once $\hat{S}(|\hat{\nabla}\hat{\psi}|)$ has been computed,

we may eliminate the pressure to arrive at the following equation for $\hat{\psi}$:

$$0 = \hat{\nabla} \cdot \left(\hat{S}(|\hat{\nabla}\hat{\psi}|) \frac{\hat{\nabla}\hat{\psi}}{|\hat{\nabla}\hat{\psi}|} \right), \tag{5}$$

as is also used in the modelling of primary cementing flows[21].

Our simulation approach proceeds as follows. First we stochastically generate a MA that is representative of the well conditions, using our existing calibrated model[1]. As there is considerable MA variation, this is repeated $N = 1000$ times for a single well, to give a distribution of MA thicknesses $\hat{H}(\hat{x}, \hat{y})$. A specific squeeze job may involve many hundreds of perforations made over a length of some metres of well. Instead, we model the invasion flow into a rectangular *tile*, surrounding a single perforation. This domain is selected for each of the N well MA considered.

The leakage flow rate is calculated for each MA before the squeeze operation. Next, the invasion flow is simulated by solving Eq. 5 on the selected computational tile. As boundary conditions we assume a fixed pressure drop between the perforation hole and the far-field. The initial concentration is $\bar{c} = 0$ everywhere in the domain and $\bar{c} = 1$ at the inflow. The slurry penetrates into the MA, stopping when the yield stress balances the driving pressure gradient, i.e. when $\hat{S} = \hat{\tau}_y/\hat{H}$. The simulation is run until $\bar{c}$ changes by $< 1\%$ between timesteps[2]. The *final* values of $\bar{c}$ are used to modify $\hat{H}(\hat{x}, \hat{y}) \mapsto [1-\bar{c}(\hat{x}, \hat{y})]\hat{H}(\hat{x}, \hat{y})$ in all parts of the MA where the squeeze operation was performed. Lastly, we recompute the leakage flow rate using the MA with the modified gap height.

The above method combines a deterministic simulation of the penetration with a stochastic generation of the $N = 1000$ MA and selection of the computational tile. The approach has been carefully developed in Izadi *et al.*[3], in particular to ensure that $N = 1000$ is sufficient to represent the variability. The most time consuming computation is the invasion flow, which is calculated by using an augmented Lagrangian formulation of Eq. 5 and iterative Uzawa algorithm, at each fixed time. The concentrations are then advected forwards by solving Eq. 1. The many iterations required at each timestep slow the procedure. This is one reason why we compute only on a single rectangular tile.

As well as comparing leakage rates before and after the squeeze job, we can analyze the effects of the squeeze job on the invasion flow, i.e. for each of the N tiles computed. There is considerable variation in the effectiveness of the invasion flow. Consequently, we instead compute the distributions of various metrics that help quantify this effectiveness. First, we calculate the minimal radius of penetration from the perforation hole: $\hat{R}_{min}$ and normalize with the distance to the boundary of the tile, to give R_{min}.

Secondly, we look at the volume fraction of the MA that remains unfilled by cement:

$$\bar{H}_{1,void} = \frac{\int_\Omega \hat{H}(1-\bar{c})\ dA}{\int_\Omega \hat{H}\ dA}, \tag{6}$$

i.e. this represents the volume remaining for the gas to flow through. Thirdly, as the overall objective of the squeeze cementing operation is to restore the well integrity, we look at a flow-based metric, $\bar{H}_{3,void}$:

$$\bar{H}_{3,void} = \frac{\int_\Omega \hat{H}^3(1-\bar{c})\ dA}{\int_\Omega \hat{H}^3\ dA}. \tag{7}$$

The point of the cubic power is that the leakage flow rates are generally low and non-inertial, hence proportional to H^3. The metric $\bar{H}_{3,void}$ thus indicates the fraction of large leakage pathways remaining open.

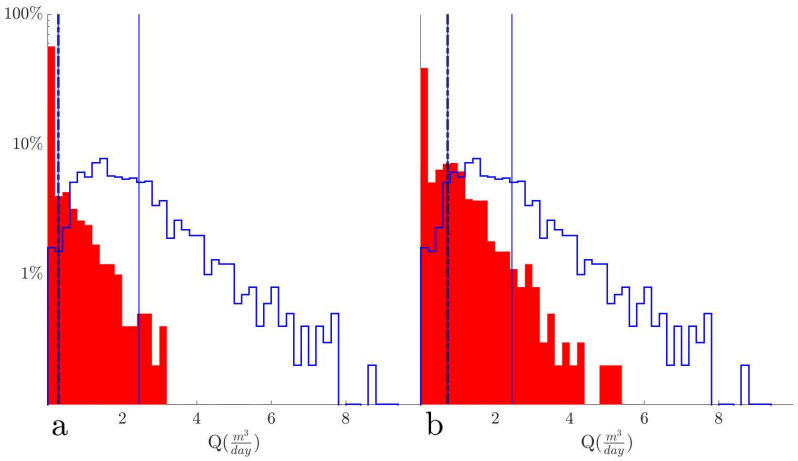

FIGURE 2: Leakage flow rate distributions before and after the squeeze job for $N = 1000$ MA constructed using $\sigma = 1.15$, $\mu = 4.1$. The blue line shows the leakage values before the squeeze job (mean leakage $\hat{\bar{Q}} = 2.44 \pm 0.11(95\%)\text{m}^3/\text{day}$. The red-filled bar charts show the leakage values after the squeeze job: a) $\hat{\tau}_Y = 0.2\text{Pa}$ and $\hat{\bar{Q}} = 0.288 \pm 0.04(95\%)\text{m}^3/\text{day}$; b) $\hat{\tau}_Y = 1\text{Pa}$ and $\hat{\bar{Q}} = 0.723 \pm 0.06(95\%)\text{m}^3/\text{day}$.

OPERATIONAL EFFECTS AND RESULTS

In Izadi *et al.*[3] we have explored the effects of the squeeze operation reducing well leakage. We have looked at different patterns of perforation shots (characterised by SPF = shots per foot), at the effects of different depths of the squeeze operation in the well, and finally at the effects of the slurry yield stress. Using a relatively thin slurry at the deepest depth (above the gas source), and with the highest shot density, all seemed to produce the best reduction in leakage rates. The effect of depth is geometric: as wells are drilled deeper their diameter decreases and hence the spacing between perforation holes in the MA is reduced.

Here we use a similar approach to study the effects of MA variability and MA thickness. As a first step we generate N=1000 microannuli based on the median BC well[1], as illustrated in **Fig. 1c**. The MA construction process for the thickness $\hat{H}(\hat{x}, \hat{y})$ randomly samples a log-normal distribution to provide seed values for $\hat{H}$ at 2 depths, which are then stochastically diffused to construct the full $\hat{H}(\hat{x}, \hat{y})$. For this we use log-normal parameters $\sigma = 1.15$, $\mu = 4.1$, which are similar to those used earlier[1].

We model the penetration into the perforated annulus, assuming a 12 SPF perforation pattern over 12m of production casing. It is assumed that leakage occurs from the production zone only. We consider squeezing using both a thin ($\hat{\tau}_Y = 0.2\text{Pa}$ yield stress) slurry and a more standard ($\hat{\tau}_Y = 1\text{Pa}$ yield stress) slurry. We compute the leakage flow rates before and after the squeeze. These are marked in blue and red in **Fig. 2**. Evidently the $\hat{\tau}_Y = 0.2\text{Pa}$ slurry is more effective than the $\hat{\tau}_Y = 1\text{Pa}$ slurry. The leakage rates (before and after) are comparable to our earlier rates[3], obtained with similar σ & μ, using $N = 2000$ MA. This establishes the results of **Fig. 2** as a reasonable baseline.

We start with exploring the effects of a thinner MA thickness, but preserve the variability of the base case. Since the MA thickness is built by randomly sampling from a log-normal, reduction of the mean MA thickness is achieved by varying the log-normal

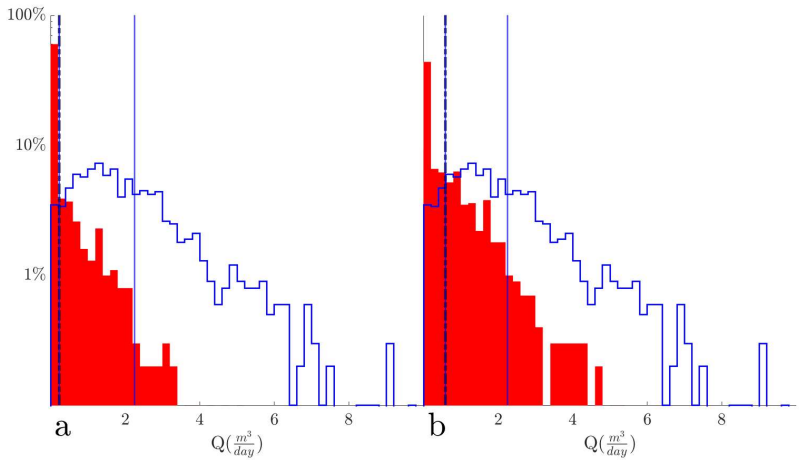

FIGURE 3: Leakage flow rate distributions before and after the squeeze job for $N = 1000$ MA constructed using $\sigma = 1.29$, $\mu = 3.7$. The blue line shows the leakage values before the squeeze job (mean leakage $\hat{\bar{Q}} = 2.25 \pm 0.11(95\%)\text{m}^3/\text{day}$. The red-filled bar charts show the leakage values after the squeeze job: a) $\hat{\tau}_Y = 0.2\text{Pa}$ and $\hat{\bar{Q}} = 0.237 \pm 0.04(95\%)\text{m}^3/\text{day}$; b) $\hat{\tau}_Y = 1\text{Pa}$ and $\hat{\bar{Q}} = 0.590 \pm 0.05(95\%)\text{m}^3/\text{day}$.

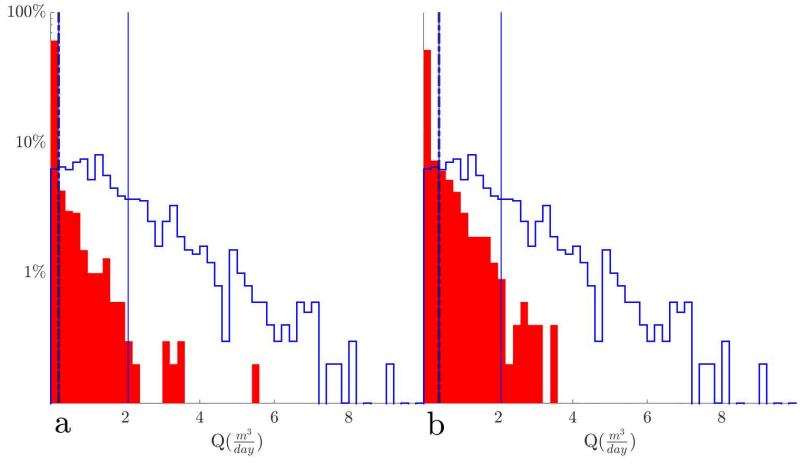

FIGURE 4: Leakage flow rate distributions before and after the squeeze job for $N = 1000$ MA constructed using $\sigma = 1.47$, $\mu = 3.17$. The blue line shows the leakage values before the squeeze job (mean leakage $\hat{\bar{Q}} = 2.09 \pm 0.12(95\%)\text{m}^3/\text{day}$. The red-filled bar charts show the leakage values after the squeeze job: a) $\hat{\tau}_Y = 0.2\text{Pa}$ and $\hat{\bar{Q}} = 0.214 \pm 0.06(95\%)\text{m}^3/\text{day}$; b) $\hat{\tau}_Y = 1\text{Pa}$ and $\hat{\bar{Q}} = 0.412 \pm 0.06(95\%)\text{m}^3/\text{day}$.

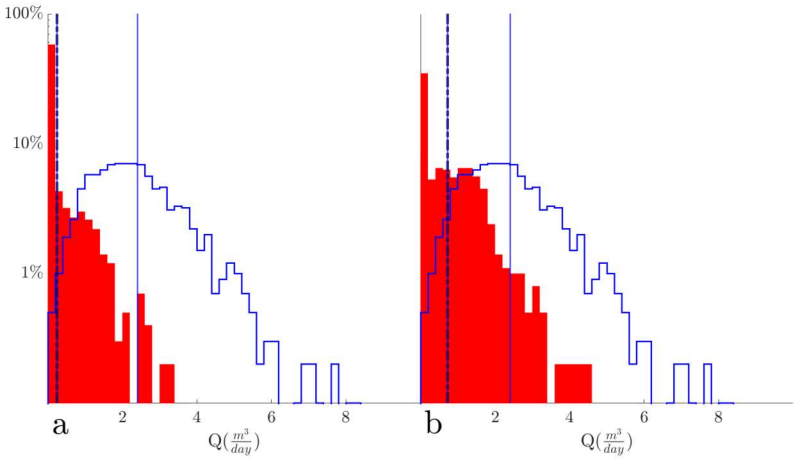

FIGURE 5: Leakage flow rate distributions before and after the squeeze job for $N = 1000$ MA constructed using $\sigma = 0.723$, $\mu = 4.5$. The blue line shows the leakage values before the squeeze job (mean leakage $\hat{\bar{Q}} = 2.4 \pm 0.08(95\%)\text{m}^3/\text{day}$. The red-filled bar charts show the leakage values before the squeeze job: a) $\hat{\tau}_Y = 0.2$Pa and $\hat{\bar{Q}} = 0.248 \pm 0.03(95\%)\text{m}^3/\text{day}$; b) $\hat{\tau}_Y = 1$Pa and $\hat{\bar{Q}} = 0.721 \pm 0.05(95\%)\text{m}^3/\text{day}$.

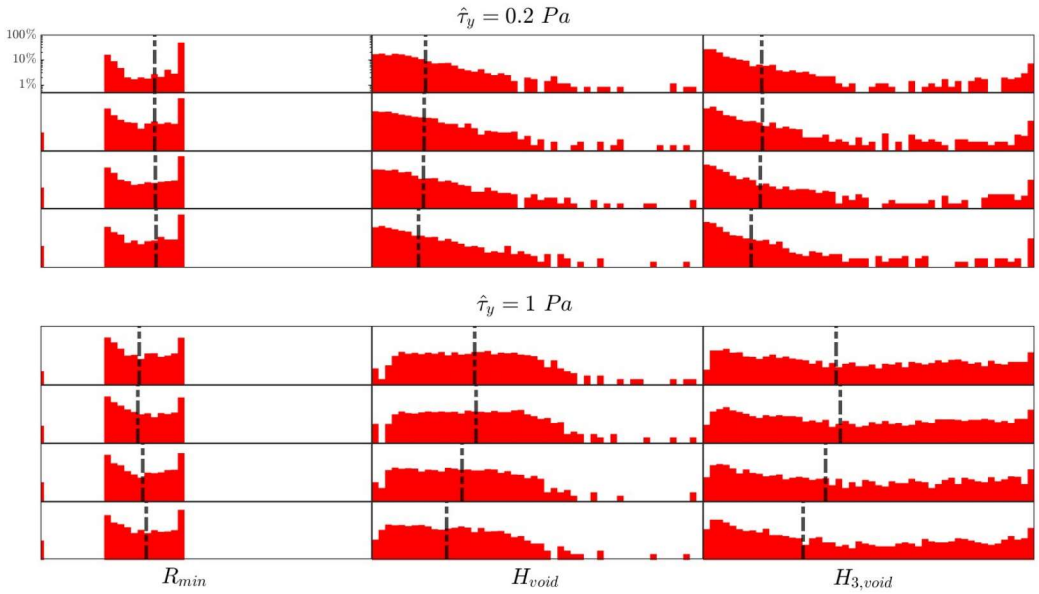

FIGURE 6: Distributions of the invasion flow metrics R_{min}, H_{void} and $H_{3,void}$. For each $\hat{\tau}_Y$ the rows 1-4 correspond to **Figs. 2-5**. Note that the each metric is normalised to be in $[0, 1]$

distribution parameters. From a physical perspective, this type of reduction might be imagined to occur for example by the use of an expanding cement or perhaps due to geological conditions affecting the water to cement ratio during hydration, reducing cement shrinkage.

Figs. 3 & **4** show the results of repeating the squeeze study with MA that have respectively 80% and 60% of the mean thickness of our base case in **Fig. 2.** The first point to note in these figures is that the reduced MA gap thickness anyway reduces the pre-squeeze leakage flow rate. However, the mean reduction is perhaps less than one might naively expect. For example, the gas flow rate scales as the cube of the gap thickness, but here with 60% of the gap thickness, the mean flow rate is not 21.6% of that in **Fig. 2.** Evidently, the larger gaps offer little resistance and this is one of the key points of including MA thickness variability in leakage models.

Again we observe that the thinner slurry penetrates better and we see a reduction in mean leakage in all cases, with a shift of the leakage distribution to the left. However, the reduced flow rate at 60% (**Fig. 4**) is not much less than that at 80% (**Fig. 3**). This is because there is a competing effect: namely, the reduced gap thickness becomes harder to penetrate, effectively this is because the critical pressure gradient $\hat{\tau}_y/\hat{H}$ increases in our invasion model. This effect is realistic for an operation pumped at a fixed control pressure. Indeed, the effects might actually be worse if the model were extended to include particle size effects and a critical shut-off due to particle jamming.

We next consider the effect of reducing the variability of the MA, but keeping the same mean thickness as in **Fig. 2.** Physically, this might result from better control of annulus eccentricity, so that the thickness of cement is more similar around the annulus. We assume that the standard deviation of the MA gap thickness is 50% of that in **Fig. 2** and repeat the analysis. The results are shown in **Fig. 5.** We see that the reduced variability of gap thickness results in significantly more effective squeeze cementing, particularly for the $\hat{\tau}_Y = 0.2$Pa slurry.

CONCLUSIONS

Largely our results here are preliminary, designed to showcase how combining the physical penetration model with the stochastic microannlus model, leads to a predictive methodology for the distribution of leakage rates. Working with a probabilistic measure seems appropriate for the high degree of uncertainty of the process. In turn, the shifts in distribution of leakage rates help us direct attention to which process parameter changes lead to robust effects on leakage.

REFERENCES

1. Trudel E., Frigaard I., Stochastic modelling of wellbore leakage in British Columbia. *J. Petr. Sci. Engng.*, **220A**, 111199, 2023

2. Izadi M., Trudel E., Chaparian E., Frigaard I., Squeeze cementing of microannuli: a viscoplastic invasion flow. *J. non-Newt. Fluid Mech.*, **319**, 105070, 2023

3. Izadi M., Trudel E., Frigaard I., Risk based analysis of squeeze cementing operations. *Geoenergy Sci. Engng.*, **234**, 212687, 2024

4. Nelson E., Guillot, D., Well cementing. Schlumberger, 2006..

5. Trudel E., Bizhani M., Zare M., Frigaard I.A., Plug and abandonment practices and trends: A British Columbia perspective. *J. Petr. Sci. Engng.*, **183**, 106417, 2019.

6. Vrålstad T., Saasen A., Fjær E, Øia T., Ytrehus J.D. and Khalifeh M., Plug and abandonment of offshore wells: Ensuring long-term well integrity and cost-efficiency. *J. Petr. Sci. Engng.*, **173**, 478–491, 2019.

7. Doherty B., Vasylkivska V., Huerta N.J., Dilmore R., Estimating the leakage along wells during geologic CO2 storage: Application of the well leakage assessment tool to a hypothetical storage scenario in Natrona County, Wyoming. *Energy Procedia*, **114**, 5151–5172, 2017.

8. Ford E.P., Moeinikia F., Lohne H.P., Arild O., Mansouri M.M., Fjelde K.K., Leakage calculated for plugged and abandoned wells. *Society of Petroleum Engineers*, SPE-185890-MS, 2017.

9. Lackey G., Vasylkivska V.S., Huerta N.J., King S. and Dilmore R.M., Managing well leakage risks at a geologic carbon storage site with many wells. *Int. J. Gr. Gas Contr.*, **88**, 182–194. 2019.

10. Willis B.M., Strutt J.E. and Eden R.D., Long term well plug integrity assurance: a probabilistic approach. *Offshore Technology Conference* OTC-29259-MS, 2019.

11. White S., Carroll S., Chu S., Bacon D., Pawar R., Cumming L., Hawkins J., Kelley M., Demirkanli I., Middleton R., Sminchak J., Pasumarti A., A risk-based approach to evaluating the area of review and leakage risks at CO2 storage sites. *Int. J. Gr. Gas Contr.*, **93**, 102884, 2020.

12. Johnson C., Sefat M.H. and Davies D., 2021. Developing a well-centric flow model. The first step in a risk-based approach to oil and gas well decommissioning. *J. Petr. Sci. Engng.*, **204**, 108651, 2021.

13. Al Ramadan M., Salehi S., Aljawad M.S. and Teodoriu C., Numerical modeling of gas migration through cement sheath and microannulus. *ACS Omega*, **6**, 34931–34944, 2021.

14. Skorpa R. and Vrålstad T., Visualization of fluid flow through cracks and microannuli in cement sheaths. *SPE Journal* **23**, 2018.

15. Vrålstad T. and Skorpa, R., Digital cement integrity: a methodology for 3D visualization of cracks and microannuli in well cement. *Sustainability*, **12**, 4128, 2020.

16. Stormont J.C., Garcia Fernandez S., Taha M.R. and Matteo E.N., Gas flow through cement-casing microannuli under varying stress conditions. *Geomech. Energy Envir.* **13**, 1–13. 2018.

17. Garcia Fernandez S., Matteo E.N., Taha M.R. and Stormont J.C., Characterization of wellbore microannuli. *J. Nat. Gas Sci. Engng.*, **62**, 13–25, 2019.

18. Corina A.N., Skorpa R., Sangesland S., Vrålstad, T., Simulation of fluid flow through real microannuli geometries. *J. Petr. Sci. Engng.* **196**, 107669, 2021.

19. Trudel E., Frigaard I., Modeling the effect of operational activity on wellbore integrity and wellbore leakage in British Columbia *Geoenergy Sci. Engng.*, **227**, 211850, 2023

20. Pelipenko S. and Frigaard I., Mud removal and cement placement during primary cementing of an oil well–Part 2; steady-state displacements. *J. Engng. Math.*, **48**, 1–26, 2004

21. Maleki A. and Frigaard I., Primary cementing of oil and gas wells in turbulent and mixed regimes. *J. Engng. Math.*, **107**, 201–230, 2017